Chemical Engineering Journal 215-216 (2013) 500–507

Contents lists available at SciVerse ScienceDirect

Chemical Engineering Journal

journal homepage: www.elsevier.com/locate/cej

Kinetics of the nopol synthesis by the Prins reaction over tin impregnated MCM-41 catalyst

Aída Luz Villa *, Luis Fernando Correa, Edwin A. Alarcón

Environmental Catalysis Research Group, Chemical Engineering Department, Universidad de Antioquia, Cra 53 N° 61-30, Medellín, Colombia

HIGHLIGHTS

- Kinetic model for nopol synthesis based on the Langmuir–Hinshelwood formalism is obtained.
- The main product, nopol, inhibits the activity of the Sn-MCM-41.
- The rate law is robust respect to equilibrium adsorption constants.
- The effect of temperature on kinetic of nopol synthesis is mainly on the surface reaction constant.

ARTICLE INFO

Article history:
Received 30 March 2012
Received in revised form 3 November 2012
Accepted 6 November 2012
Available online 12 November 2012

Keywords:
Nopol
Sn-MCM-41
Prins reaction
Kinetic model
Reaction mechanism

ABSTRACT

The kinetics of the nopol synthesis by Prins condensation of β-pinene and paraformaldehyde over Sn-MCM-41 synthesized by impregnation was evaluated using the initial reaction rate method. The reaction rate equation obtained from a kinetic model based on the Langmuir–Hinshelwood formalism with the surface reaction of adsorbed reactants on catalytic sites of the same nature as the limiting step, gave a good prediction of the experimental data. The effect of temperature on the kinetics of nopol synthesis over Sn-MCM-41 obtained by impregnation was studied between 75 and 100 °C. The robustness analysis of the kinetic model showed that the surface reaction constant, k'_{sr}, should be about 0.185 mol g^{-1} h^{-1} at 90 °C, while the ratio between the adsorption equilibrium constant of β-pinene, K_A, and formaldehyde species, K_B, is approximately 1.2:1 (K_A:K_B). The obtained apparent activation energy and pre-exponential factor are 78 kJ/mol and 2.3 × 10^{10} mol g^{-1} h^{-1}, respectively, but compensation effect analysis using both experimental and simulated data gave strong evidence of the dependency in temperature of the apparent Arrhenius parameters.

1. Introduction

Nopol is an optically active, unsaturated and bicyclic monoterpenic alcohol obtained from natural β-pinene and it is useful as a raw material for synthesis of fragrances and household products [1]. Nopol is produced from the Prins condensation of β-pinene and paraformaldehyde under anhydrous conditions at temperatures above 180 °C or using $ZnCl_2$ as homogeneous catalyst [2]. Recently, high nopol yields were reported over tin supported MCM-41 [3–7] and SBA-15 [8,9] materials. Sn-MCM-41 synthesized by impregnation of $SnCl_2{\cdot}2H_2O$ in an ethyl acetate dissolution under incipient wetness conditions, exhibits higher activity that Sn-MCM-41 materials obtained by CVD of $SnCl_4$, with the additional advantage that its regeneration is possible by exhaustive washing with acetone instead of thermal treatment under air atmosphere [10]. These promising results encouraged our research group to carry out kinetic studies as they are useful for reactor design purposes and for better understanding of the phenomena related to nopol production. No detailed kinetic studies have been reported for the production of nopol or another α, β-unsaturated alcohol obtained neither by the Prins reaction over heterogeneous catalytic conditions nor under homogeneous acid catalyzed reactions. In the absence of catalyst, Watanabe [11] reported reaction rate of first order respect to each reactant for nopol synthesis at temperatures between 170 and 190 °C. The reaction rate law reported over Sn-SBA-15 was of pseudo-first order [8]. Using Sn-MCM-41 prepared by impregnation [12], with a pseudo-homogeneous rate law determined by the excess method [13], zero and second order respect to β-pinene and formaldehyde, respectively, were obtained. As the rate laws reported for those heterogeneous catalytic systems were not based on a mechanism that included the characteristic adsorption phenomena step of the heterogeneous catalytic phenomena, in this contribution a reaction mechanism based on the Langmuir–Hinshelwood formalism is proposed for nopol synthesis over Sn-MCM-41 material obtained by impregnation. Initial reaction

* Corresponding author. Tel.: +574 2196609.
E-mail address: alvilla@udea.edu.co (A.L. Villa).

1385-8947/$ - see front matter © 2012 Elsevier B.V. All rights reserved.
http://dx.doi.org/10.1016/j.cej.2012.11.030

rates for nopol synthesis were estimated under several reactant concentrations and at temperatures between 75 and 100 °C.

2. Experimental

2.1. Catalyst synthesis

Tin supported MCM-41 material was synthesized by incipient wetness impregnation following previously reported procedures [10]. The support (2 g), synthesized according to the method developed by Grün et al. [14], was mixed with 3 mL of a solution of $SnCl_2{\cdot}2H_2O$ in ethyl acetate (28.7 μmol Sn/mL) under inert atmosphere, then the solvent was allowed to evaporate for 24 h at room temperature; finally, the solid was calcined at 550 °C for 5 h. The material was coded as Sn(0.28)-I, where the number in parentheses corresponds to the tin weight percent loading determined by atomic absorption.

2.2. Catalytic tests

The reactions were performed in 2 mL capped vials covered with inert silicone septa and immersed in an oil bath which temperature was controlled with an IKA fuzzy controller, and the stirring rates of the stir plate were calibrated and measured with an Extech Instrument digital stroboscope. The catalytic tests were carried out at least by duplicate in six batch reactors under identical reaction conditions (Fig. 1 and Table 1), that is, 1 mg of catalyst Sn(0.28)-I, 1 mL of β-pinene in toluene solution at a concentration between 0.063 and 0.5 M, and paraformaldehyde (0.046–2.5 M). Each reactor was removed from the oil bath every 5 min and cooled immediately with pressurized air, then the solid and the liquid phases were separated by centrifugation. The size of the catalyst was classified with standard series mesh of 170, 270, 325 and 400. The particle size distribution was measured with laser diffraction using a Master Sizer 2000 ver. 5.6 (model Hydro 2000S AWA, Malvern Instruments Ltd., UK) on solids dispersed in water under ultrasound. Table 2 shows the properties of the sieved solids. The temperature effect on the nopol production was evaluated between 75 and 100 °C, with increases of 5 °C (Table 3). The reaction products in the liquid phase were identified in a GC–MS Agilent 7890 N equipped with a HP-5 capillary column, FID detector and autosampler. The carrier gas was He (1 mL min^{-1}) and the split ratio 100:1. The oven temperature was kept at 90 °C for 1 min and then it was raised to 160 °C at 10 °C min^{-1} for 7 min. The quantification of nopol and β-pinene was carried out by multi point calibration curves using dodecane as internal standard. The initial reaction rates of β-pinene disappearance and nopol formation were determined from the slopes of the curves of concentration of the corresponding compound against the time evaluated at $t = 0$.

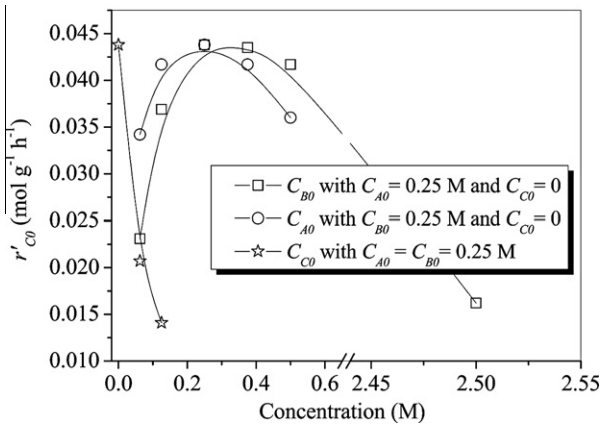

Fig. 1. Effect of the concentrations of reagents on the initial reaction rate of nopol formation, r'_{C0}.

3. Results and discussion

3.1. Mass transfer considerations

The reaction conditions that avoided mass transfer limitations were determined. Particle sizes estimated by the average between standard meshes are in good agreement with those values obtained by the particle size distribution analyzer. Average particle size below 38 μm, could actually correspond to particles of 33.4 μm and lower. To evaluate the effect of external diffusion on the reaction rate, the reaction was carried out at different stirring rates (650–2000 rpm) under standard reaction conditions and with a fixed average particle size of 41.5 μm (Fig. 2). The highest initial reaction rate was obtained above 2000 rpm. The effect of the internal diffusion on the reaction rate was evaluated by changing the average particle size (38–71.5 μm) under the standard reaction conditions and at a stirring rate of 2000 rpm (Fig. 2). These results indicated that the initial reaction rate is almost constant when the average particle size of the catalyst is between 38 and 41.5 μm. Thus, all further experiments were carried using catalyst with an average particle size of 38 μm and at a stirring rate of 2000 rpm.

3.2. Determination of the kinetic rate law

Table 1 shows the effect of the substrate concentrations on the experimental initial reaction rates of β-pinene disappearance and nopol formation. Although, the results suggest that parallel reactions of β-pinene take place from the starting of the reaction, since $-r'_{A0} \geqslant r'_{C0}$, for next analysis only nopol production is taken into account. Side product formation was favored over Sn(0.28)-I with a large excess of β-pinene or paraformaldehyde (runs 1 and 6). We previously reported that byproducts from isomerization of β-pinene, such as camphene and limonene, and from allylic oxidation such as myrtenol, are observed at high conversions (above 60%) over Sn-MCM-41 obtained by chemical vapor deposition (CVD) or by direct hydrothermal synthesis [6]. Over Sn(0.28)-I not only the aforementioned byproducts but also nopyl acetate, pinocarveol and myrtenyl acetate byproducts were observed.

Fig. 1 shows the effect of the concentration of reactants on the initial reaction rate of nopol formation. The decrease of the initial reaction rate in the presence of nopol suggests a strong adsorption of the main reaction product on active catalytic sites. A maximum in the r'_{C0} was observed in the absence of nopol in the initial reaction mixture and under stoichiometric conditions. The type of profile obtained is typical of bimolecular processes where the two reactants are adsorbed in one kind of site [15], which corresponds to mechanism 1 (Table 4). The model M1 had the best fitting of the experimental data (higher R^2, lower RSS and MSE, with randomly distribution of residuals); the predicted initial rate is showed in Fig. 3. Model M1 was obtained from the mechanism 1 according to the Langmuir–Hinshelwood formalism, where the surface reaction was assumed as the rate determining step, as it is the case of the most of heterogeneous catalytic reactions [13,15]. The mechanism 2 and its corresponding model M2 are included for comparison, but it is clear from its statistics that the experimental data fitting is not better than for model M1.

3.3. Sensibility analyses of the kinetic parameters of model M1

The constants determined with the nonlinear regression of model M1 at 90 °C were $k'_{sr} = 0.185 \pm 0.009$ mol g^{-1} h^{-1},

Table 1
Effect of the concentration of β-pinene, paraformaldehyde and nopol on the initial reaction rate of β-pinene disappearance and nopol formation.

Run	Concentration (M)			$r'_{i0} \pm SD$(mol g^{-1} h^{-1})	
	β-pinene (A)	HCHOx (B)	Nopol (C)	$-r'_{A0}$	r'_{C0}
1	0.250	0.063	0	0.0621 ± 0.0040	0.0232 ± 0.0030
2	0.250	0.125	0	0.0424 ± 0.0050	0.0370 ± 0.0060
3	0.250	0.250	0	0.0580 ± 0.0010	0.0438 ± 0.0010
4	0.250	0.375	0	0.0587 ± 0.0010	0.0436 ± 0.0005
5	0.250	0.500	0	0.0468 ± 0.0060	0.0416 ± 0.0010
6	0.250	2.500	0	0.0312 ± 0.0080	0.0162 ± 0.0040
7	0.063	0.250	0	0.0411 ± 0.0070	0.0343 ± 0.0020
8	0.125	0.250	0	0.0509 ± 0.0020	0.0418 ± 0.0005
9	0.375	0.250	0	0.0574 ± 0.0030	0.0418 ± 0.0020
10	0.500	0.250	0	0.0372 ± 0.0005	0.0359 ± 0.0030
11	0.463	0.046	0	0.0416 ± 0.0020	0.0186 ± 0.0030
12	0.250	0.250	0.0625	0.0291 ± 0.0100	0.0206 ± 0.0030
13	0.250	0.250	0.125	0.0270 ± 0.0030	0.0139 ± 0.0030

r'_{i0}: initial reaction rate of disappearance of β-pinene, $-r'_{A0}$, and formation of nopol, r'_{C0}; SD: experimental standard deviation.

Table 2
Particle size properties of sieved materials.

Sieve range	Average particle size (μm)[a]	Percentile 0.90 (μm)[b]
170–270	71.5	71.7
270–325	49.0	47.9
325–400	41.5	43.1
<400	<38	33.4

[a] Average between sizes of standard series mesh.
[b] Indicates the highest size of 90% of the analyzed particles using a Master Sizer.

Table 3
Temperature effect on the measured initial reaction rate of nopol production.

Run	Temperature (°C)	$r'_{C0} \pm$ SD (mol g^{-1} h^{-1})
1	75	0.0090 ± 0.0010
2	80	0.0172 ± 0.0016
3	85	0.0216 ± 0.0014
4	90	0.0402 ± 0.0010
5	95	0.0473 ± 0.0039
6	100	0.0534 ± 0.0033

Reaction conditions: 1.0 mL of β-pinene in toluene solution (0.25 M), β-pinene: HCHOx molar ratio of 1:2, 1 mg catalyst.

$K_A = 126 \pm 35$ M^{-1}, $K_B = 105 \pm 29$ M^{-1} and $K_C = 401 \pm 4 \times 10^{-8}$ M^{-1}. The K_A:K_B ratio is about 1.2:1, and independently of the values of the adsorption constants, if that ratio is maintained, the predicted initial reaction rate of nopol formation does not vary (Fig. 3). This sensitivity analysis is a first indication of the robustness of the model that would indicate that: (i) it could be possible to determine one adsorption constant at 90 °C if the experimental value of the other constant is known; and (ii) the temperature effect could be only determined on the rate constant of the surface reaction, k'_{sr}. The sensibility analysis of the reaction parameters of the model M1 was carried out with concentrations of β-pinene and paraformaldehyde of 0.25 M and 0.5 M, respectively, without nopol addition, at 90 °C, with $r'_{C0} = 0.0423$ mol g^{-1} h^{-1}. This value was compared to the value of r'_{C0} recalculated, $(r'_{C0})_{rc}$, after some modifications: (i) changing k'_{sr} in some percent and maintaining the $K_A/K_B = 1.2$, (ii) varying K_A (or K_B) and maintaining both $K_A/K_B = 1.2$ and $k'_{sr} = 0.185$ mol g^{-1} h^{-1} (continuous lines in Fig. 4), and (iii) modifying K_A/K_B maintaining $k'_{sr} = 0.185$ mol g^{-1} h^{-1} (Fig. 4, dashed line). These results indicate that the initial reaction rate of nopol production is proportional to changes in k'_{sr}. A simultaneous variation in both K_A and K_B up to 500%, or even higher, produced a maximum change in the initial reaction rate of nopol production of about 2%, confirming the robustness of the model respect to these parameters.

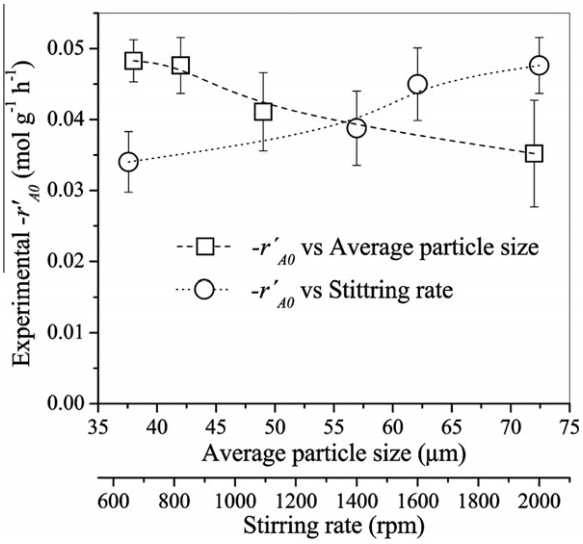

Fig. 2. Effect of the average particle size and the stirring rate on the initial reaction rate (disappearance) of β-pinene, $-r'_{A0}$, to evaluate the mass transfer resistances. Reaction conditions: 1.0 mL of β-pinene in toluene solution (0.25 M), β-pinene: HCHOx molar ratio of 1:2, 90 °C, 1 mg catalyst; 2000 rpm (□) and an average particle size of 42 μm (○).

3.4. Temperature effect on the reaction rate law

The adsorption equilibrium constant dependency on temperature is given by the Van't Hoff equation, Eq. (1) [16]. If $\Delta H_{ads,i}$ is not strongly temperature-dependent between T_1 and T_2, then Eq. (1) is transformed into Eq. (2). At the reference temperature ($T_1 = 90$ °C) $K_{A,T1}/K_{B,T1} = 1.2$, the ratio $K_{A,T2}/K_{B,T2}$ is calculated according to Eq. (3). Fig. 5 shows that $K_{A,T2}/K_{B,T2} \approx K_{A,T1}/K_{B,T1}$ if the adsorption enthalpies of both reactants were similar. Although changes up to 300% were possible in the ranges of temperature and differences of adsorption enthalpies analyzed, Fig. 4 would give a maximum variation of around 10% in the initial reaction rate of nopol production. Under these analyses, we propose that the effect of temperature on reaction rate could be mainly considered on the surface reaction constant.

$$\frac{d\ln K}{dT} = \frac{\Delta H_{ads}}{RT^2} \tag{1}$$

$$K_{i,T_2} \approx K_{i,T_1} \exp\left[-\frac{\Delta H_{ads,i}}{R}\left(\frac{1}{T_2} - \frac{1}{T_1}\right)\right] \tag{2}$$

$$\frac{K_{A,T_2}}{K_{B,T_2}} = \frac{K_{A,T_1}}{K_{B,T_1}} \exp\left[-\frac{(\Delta H_{ads,A} - \Delta H_{ads,B})}{R}\left(\frac{1}{T_2} - \frac{1}{T_1}\right)\right] \tag{3}$$

In order to assess the validity of our proposal, available kinetic data of heterogeneously catalyzed reactions with a rate law similar to model M1 in a liquid phase were analyzed, Table 5 [17–21]. These reactions include alkylation [17], oxidation [18], and hydrogenation [19–21]. Table 5 shows that the K_A/K_B ratio decreases when the temperature increases, as it is concluded from Eq. (3). Unfortunately, it was not possible to confirm that the observed effect of temperature on $\Delta r'_{C0}$ is of the same order of magnitude of $\Delta k'_{sr}$, because there were not enough available data in those references to carry out the calculations. However, the $|\Delta H_{ads,A} - \Delta H_{ads,B}|$ varied between 4.0 and 115.8 kJ/mol [17–27]. We chose a

Table 4
Statistics of the best fitted reaction rate law of nopol synthesis ($A + B \rightarrow C$) and their mechanisms.

Mechanism	Rate law	Parameters	Value	IC	R^2 (RSS, MSE)
Mechanism 1					
$A + S \overset{k_A}{\leftrightarrow} A \cdot S$ (1)	Model M1 $\cdot\ r'_C = \frac{k'_{sr} K_A K_B C_A C_B}{(1+K_A C_A + K_B C_B + K_C C_C)^2}$	k'_{sr}	0.185	0.009	0.9178
$B + S \overset{k_B}{\leftrightarrow} B \cdot S$ (2)		K_A	126.0	35.0	$(1.2 \times 10^{-5}, 2.6 \times 10^{-4})$
$A \cdot S + B \cdot S \overset{k_{sr}}{\rightarrow} C \cdot S + S$ (3)[a]		K_B	105.2	29.1	
$C \cdot S \overset{k_C}{\leftrightarrow} C + S$ (4)		K_C	400.6	4×10^{-8}	
Mechanism 2					
$A + S \overset{k_A}{\leftrightarrow} A \cdot S$ (1)	Model M2 $\cdot\ r'_C = \frac{k'_{sr} K_A K_B C_A C_B}{(1+K_A C_A)(1+K_B C_B + K_C C_C)}$	k'_{sr}	0.0392	0.0043	0.4641 (7.6×10^{-5}, 0.001681)
$B + L \overset{k_B}{\leftrightarrow} B \cdot L$ (2)		K_A	3942	6×10^{-9}	
$A \cdot S + B \cdot L \overset{k_{sr}}{\rightarrow} C \cdot L + S$ (3)[a]		K_B	41.3	9×10^{-6}	
$C \cdot L \overset{k_C}{\leftrightarrow} C + L$ (4)		K_C	136	2×10^{-6}	

[a] Rate determining step. r'_C: Initial reaction rate of nopol formation (mol g^{-1} h^{-1}), C_i: initial concentration of each specie i, k_{sr}: surface reaction constant, K_i: adsorption constant for each specie i ($K_i = k_i/k_{-i}$), A: β-pinene, B: paraformaldehyde, C: nopol, $k'_{sr} = k_{sr} \cdot \rho$, ρ: concentration of active sites on the catalyst surface (mol g^{-1}). IC: 95% confidence interval. R^2: determination coefficient. RSS: residuals sum of squares. MSE: mean squared error. The nonlinear regressions were carried out in Statgraphics 5.1.

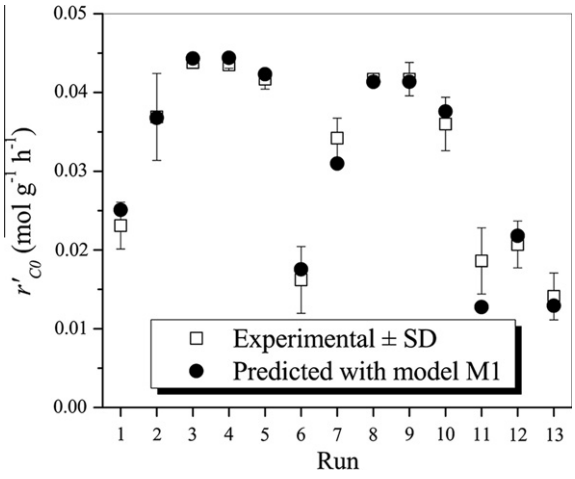

Fig. 3. Experimental and predicted data with model M1. Reaction conditions of runs are in Table 1.

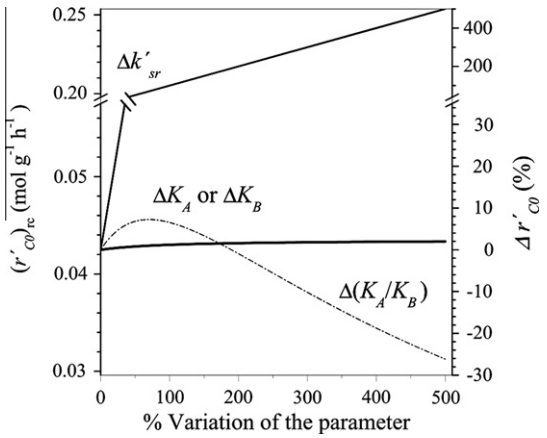

Fig. 4. Sensibility analysis of the constants of model M1 showed in Table 4. $\Delta r'_{C0} = [(r'_{C0})_{rc} - r'_{C0}]/r'_{C0} * 100\%$, where $r'_{C0} = 0.0423$ mol g^{-1} h^{-1} at 90 °C. $k'_{sr} = 0.185$ mol g^{-1} h^{-1}, $K_A = 126$ M^{-1} and $K_B = 105$ M^{-1}.

$|\Delta H_{ads,A} - \Delta H_{ads,B}|$ of 115 kJ/mol and together with the estimated Arrhenius parameters, the effect of $\Delta k'_{sr}$ and $\Delta(K_A/K_B)$ on $\Delta r'_{C0}$ was determined for nopol synthesis under the reaction conditions used in this research.

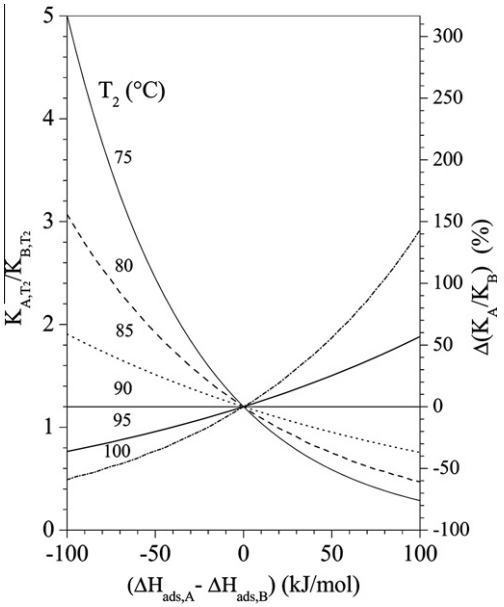

Fig. 5. Effect of the adsorption heat differences of β-pinene and formaldehyde species between 75 and 100 °C. $\Delta(K_A/K_B) = (K_{A,T2}/K_{B,T2} - 1.2)/1.2 * 100\%$.

For obtaining the Arrhenius parameters, the surface reaction constants were determined between 75 and 100 °C, with the experimental data of the initial reaction rate production of nopol (Table 3) and with following equation:

$$k'_{sr} = \frac{r'_{C0}(1 + K_{A,T_1} C_{A0} + K_{B,T_1} C_{B0})^2}{K_{A,T_1} K_{B,T_1} C_{A0} C_{B0}} = k'' r'_{C0} \quad (4)$$

where r'_{C0} is the initial reaction rate of nopol production, C_{A0}:C_{B0} = 1:2, $K_{A,T1}$ = 126 M^{-1}, $K_{B,T1}$ = 105 M^{-1}, and k'' = 4.37.

Fig. 6 shows the Arrhenius plot of the reaction rate constant of nopol production over Sn-MCM-41, and the reaction carried out without catalyst and without solvent that was reported by Watanabe [11]. Table 6 shows the corresponding Arrhenius parameters, i.e. apparent pre-exponential factor, A_{app}, and the apparent activation energy, E_{app}, for nopol production by thermal synthesis and heterogeneous catalytic processes over Sn-MCM-41 and Sn-SBA-15. The apparent activation energies of the heterogeneous Sn-MCM-41 and the non-catalyzed system were around of 67 and 79 kJ/mol, respectively, without considering the constant value at

Table 5
Effect of temperature on the parameters of the rate law of liquid phase reactions which kinetic expression analogous to model M1.

Rate law expression, [a] $-r'_i$	T_0 (K)	ΔT (K)[b]	$\Delta k'_{sr}$, (%) [b]	$\Delta(K_A/K_B)$ (%) [b]	$\lvert\Delta H_{ads,A} - \Delta H_{ads,B}\rvert$ (kJ/mol)[b]	Ref.
$-r_A = \frac{k_1 K_A K_B C_A C_B}{(1+K_A C_A+K_B C_B+K_C C_C)^2}$	313	10	55.7	−8.5	7.3	[17]
A: *tert*-butyl alcohol		20	136.7	−15.6		
B: phenol		30	248.1	−22.0		
C: *p*-*tert*-butyl phenol						
$-r_A = \frac{k_{ST} K_A^{0.5} K_B C_A^{0.5} C_B}{(1+K_A^{0.5} C_A^{0.5}+K_B C_B)^2}$	423	25	183.7	−33.0	16.8	[18]
A: oxygen		40	736.6	−9.1		
B: total organic carbon (TOC)		50	1821.5	−2.1		
$-r_{IV} = \frac{K_S K'_{H2} K_{IV} P_{H2} C_{IV}}{(1+K'_{H2} P_{H2}+K_{IV} C_{IV})^2}$	393	15	72.3	−14.9	115.8	[19]
H_2: hydrogen		30	278.1	−92.1		
IV: iodine value of palm fatty acid						
$-r_R = \frac{L k_{r1} K_R K_{H2} C_R P_{H2}}{(1+K_R C_R+K_{H2} P_{H2})^2}$	323	30	283.3	−35.0	15.8	[20]
R: Citral		40	455.6	−45.3		
H_2: hydrogen						
$-r_{COD} = \frac{k_1 K_{COD} K_{H2} C_{COD} C_{H2}}{(1+K_{COD} C_{COD}+K_{H2} C_{H2})^2}$	313	10	100.0	−38.2	54.6	[21]
COD: 1,5-cyclooctadiene		30	1233.3	−82.5		
H_2: hydrogen						

T_0 is the lowest temperature reported in the reference.
$\Delta T = (T - T_0)$.
$\Delta k'_{sr} = ((k'_{sr,T} - k'_{sr,T0})/k'_{sr,T0}) * 100\%$.
$\Delta(K_A/K_B) = ((K_{A,T}/K_{B,T}) - (K_{A,T0}/K_{B,T0})) * 100\%/(K_{A,T0}/K_{B,T0}))$.
$\lvert\Delta H_{ads,A} - \Delta H_{ads,B}\rvert$ is the absolute value of the difference between enthalpies of adsorption.
[a] The component A was chosen in order to have $\lvert\Delta H_{ads,A}\rvert > \lvert\Delta H_{ads,B}\rvert$.
[b] Determined with data from the reference.

75 °C, since this value is out of the trend, attributed to the fact that below 80 °C the paraformaldehyde depolymerization rate toward its monomeric units of HCHO is low [28].

On the other hand, if Arrhenius parameters of Table 6 are taken along with the hypothetical $\lvert\Delta H_{ads,A} - \Delta H_{ads,B}\rvert$ = 115 kJ/mol, Fig. 7 is obtained using $k'_{\text{simulated}}$ from Eq. (4). Simulated data indicate only pronounced deviations at 100 °C, suggesting that our hypothesis is a good approximation for the lowest temperatures on this work. Moreover, simulated data have a good fit to a second order polynomial. Experimental data for nopol kinetics (Fig. 6) and the data reported by Ramaswamy [8] seem to have also this shape. Lyngaard et al. [16] reported the compensation effect in the apparent activation energy and pre-exponential factor with temperature. It means that $\ln r'_{C0}$ vs. $1/T$ or $(\ln k'_{sr} - \ln k'')$ vs. $1/T$ are not linear functions and Eqs. (5) and (6) are valid, were a and b are known as the linear parameters of Cremer–Constable relation [16]:

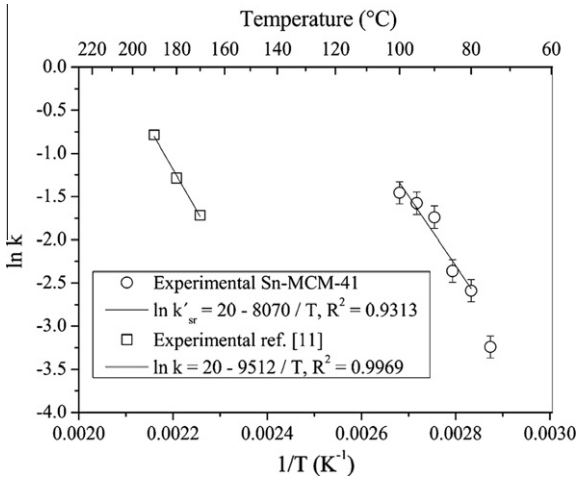

Fig. 6. Temperature effect on the reaction rate constant of nopol production without catalyst [11] and over Sn-MCM-41 synthesized by impregnation.

$$E_{app} = -R\frac{d(\ln r'_{C0})}{d(1/T)} = -R\frac{d(\ln k'_{sr})}{d(1/T)} = RT^2\frac{d(\ln k'_{sr})}{d(T)} \quad (5)$$

$$\ln A_{app} = \frac{E_{app}}{RT} + \ln r'_{C0} = a^* E_{app} + b \quad (6)$$

Taking into account the observed second order polynomial dependency respect to $1/T$ discussed above, the Eq. (7) is obtained for temperatures between 75 and 100 °C. The temperature dependency of E_{app} and the Constable plot are displayed in Figs. 8 and 9, respectively. Although the apparent activation energy average obtained from the Constable plot (77 kJ/mol) is very close to the value obtained from linear approximation (Table 6), Fig. 8 shows that the E_{app} varies between 28 and 128 kJ/mol, showing the temperature effect on this parameter:

$$\ln k'_{sr} = -218.05 + 164939.15\frac{1}{T} - 31383471.82\frac{1}{T^2}, \quad R^2 = 0.98185 \quad (7)$$

3.5. Comparison of the proposed kinetics with another reports based on heterogeneous catalysis

Table 6 (entry 3) shows the Arrhenius parameters reported for the nopol production over Sn-SBA-15 [8], giving an activation energy of around 47 kJ/mol The data reported over Sn-SBA-15 were obtained at 70, 80, 90 and 110 °C [8], and between 2 and 24 h. Our experimental rate data obtained at 90 °C [10] were correlated with the integral method in a similar way as Sn-SBA-15, producing also a pseudo-first order kinetic respect to β-pinene (Fig. 7, dashed lines). The determination coefficients, R^2, were reasonably high (96–99%), excepting the data that correspond to a catalyst and β-pinene concentration of 1 mg/mL and 0.25 M, respectively.

For determining if the kinetic model M1 is coherent with experimental data, Eqs. (8)–(12) were used. Eq. (8) corresponds to the mole balance of nopol in a batch reactor and Eq. (9) to the yield definition:

$$r_C W = \frac{dN_C}{dt} \quad (8)$$

Table 6
Arrhenius parameters reported for nopol synthesis with several systems.

Entry	System or catalyst	Method used for rate data analysis	Rate law	E_{app} (kJ/mol)	A_{app}	Ref.
1	Sn-MCM-41	Initial reaction rates	Eq. (4)	67 ± 10 (78 ± 9) [a]	6.52×10^8 mol g^{-1} h^{-1}	This work
2	Thermal synthesis	No available	$k = \frac{r_C}{C_A C_B}$	79 ± 4	3.8×10^8 mol^{-1} h^{-1}	[11]
3	Sn-SBA-15	Pseudo-first order fitted to data between 2 and 24 h	$k' = \frac{r_C}{C_A}$	47 ± 9[b]	5.3×10^5[c]	[8]

[a] Determined between 80 and 100 °C; in parenthesis E_{app} in the range 75–100 °C.
[b] Calculated value from the reported Arrhenius plot.
[c] Units not available.

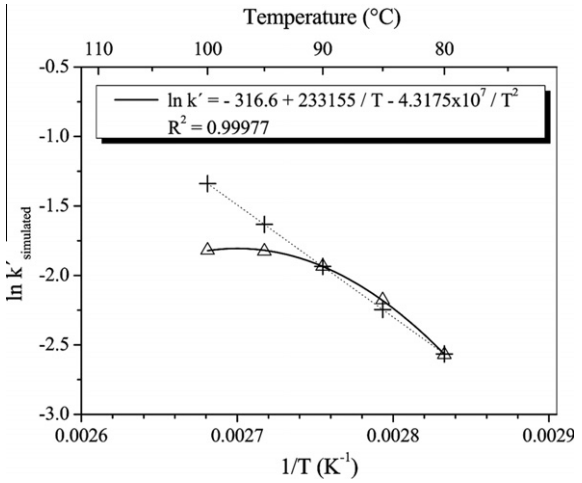

Fig. 7. The effect of temperature simulated with Eq. (4) using the estimated Arrhenius parameters and hypothetical difference of adsorption enthalpies. Arrhenius parameters from Table 6 (+ dashed lines), simulated data (Δ), and polynomial fitting (continuous line).

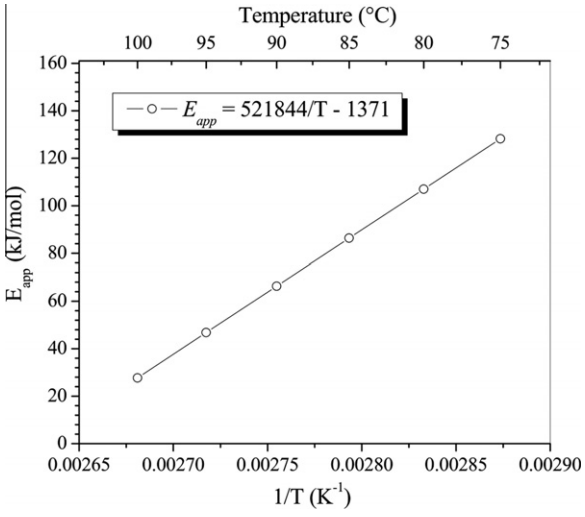

Fig. 8. Effect of temperature in the apparent activation energy.

$$N_C = N_{A0} Y \tag{9}$$

Eq. (10) gives a correlation between the fractional conversion of β-pinene (X) and the amount of catalyst (W) with the nopol yield (Y), according to experimental data showed in Fig. 9 [10], with R^2 = 99.5%.

$$Y = 0.8517X - 0.1770W \tag{10}$$

Eq. (11) was obtained after calculation with a fixed catalyst weight. Eq. (12) was obtained by replacing the kinetics of nopol synthesis given by model M1 in following equation:

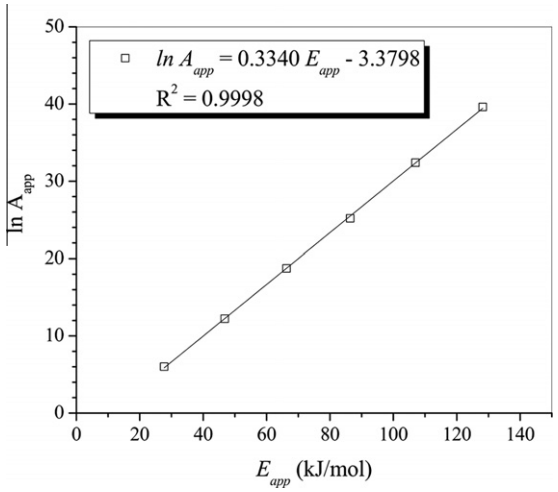

Fig. 9. Constable plot for variation in apparent prefactors due to temperature changes.

$$r'_C W = 0.8517 N_{A0} \frac{dX}{dt} \tag{11}$$

$$\frac{dX}{dt} = \frac{k'_{sr} K_A K_B C_{A0}^2 (1-X)(\theta - X)}{(1 + K_A C_{A0}(1-X) + K_B C_{A0}(\theta - X) + K_C C_{A0} X)^2} * \frac{W}{N_{A0}} \times \frac{1}{0.8517} \tag{12}$$

The simulation of Eq. (12), with constants of mechanism 1, was carried out using ODE45 tool from Matlab (Fig. 10, continuous lines), indicating that the simulated data also have a good fit with a kinetic of a pseudo-first order after 2 h of reaction. The simulation of Eq. (12) at different temperatures, with the Arrhenius parameters in Table 6, produced apparent activation energy around 58 kJ/mol (vs. 67 kJ/mol). It means lower activation energies could be predicted if the pseudo-homogeneous rate laws were used, as observed in Table 6.

In contrast with the good fit at initial rates (Fig. 3), some discrepancies between the experimental data and the predicted values by Eq. (12) at long reaction times are observed in Fig. 10; those differences may be owing to nopol deactivation as it is suggested in model M1. We use a semi-empirical deactivation kinetic approach, Eq. (13) [13], and an independent poisoning, Eq. (14) [29], that gave a good fitting of the experimental data (Fig. 11). The best parameters found were: first order deactivation kinetics (n = 1), asymptotic activity a^* = 0 and deactivation constant k_d = 0.1838 h^{-1}. Although, the trend is improved up to 9 h, there is still a lack of fit at 24 h. A phenomenological interpretation of all processes occurring in the reactor at long times is under progress in our laboratory in order to understand the behavior of the catalytic system and to improve the predictability of the model. The possible processes are: (i) a competitive adsorption of reactants and byproducts over the active sites; (ii) depolymerization

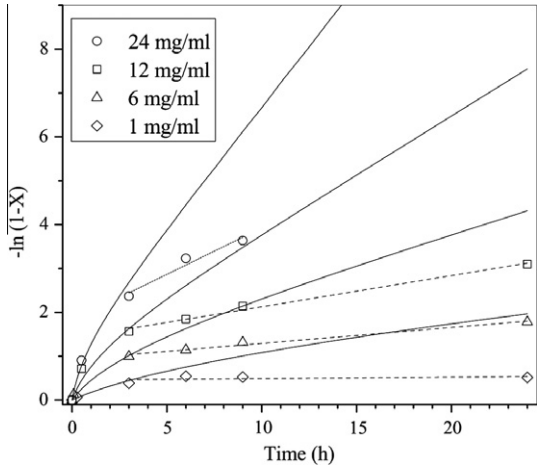

Fig. 10. Experimental (symbols) and simulated data with Eq. (12) (continuous lines). Reaction conditions: catalyst (1–24 mg), β-pinene in toluene solution 0.46 M (1 mL), paraformaldehyde: β-pinene ratio of 2:1, 90 °C. β-pinene solution was 0.25 M when the catalyst concentration was 1 mg/mL.

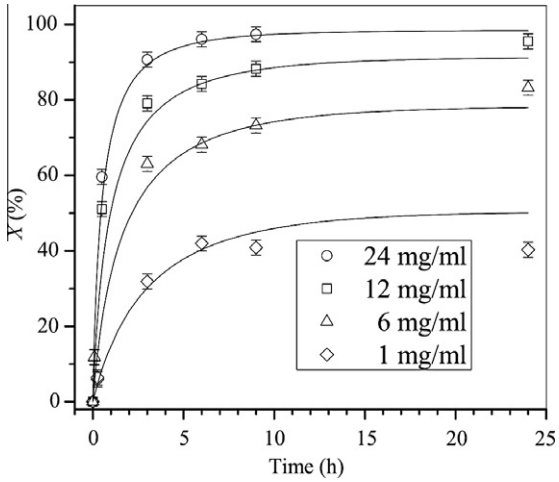

Fig. 11. Experimental and simulated data with Eqs. (12)–(14). Reaction conditions as in Fig. 10.

of paraformaldehyde to formaldehyde, above 80 °C [28]; (iii) diffusion of solubilized HCHO throughout pores and active sites of the solid catalyst; and (iv) competitive reactions of gaseous HCHO on the colder zones of the reactor, which depends on the reaction system setup [30]:

$$a(t) = \frac{-r_i(t)}{-r_i(t=0)} \tag{13}$$

$$\frac{da}{dt} = -k_d(a - a^*)^n \tag{14}$$

4. Conclusions

A model deduced from a mechanism where the determining reaction rate step is the surface reaction between aldehyde species and β-pinene, both adsorbed on sites of the same nature, with the later desorption of the product is coherent with the experimental data under initial rate conditions. The model predicts a catalyst inhibition by the adsorption of the produced nopol. At 90 °C the relation among the adsorption constants K_A and K_B in the model M1 (A: β-pinene, B: paraformaldehyde) is about 1.2:1. A sensibility analysis of the model confirmed its robustness when the K_A:K_B ratio is kept constant around 1.2, allowing an easier analysis of the temperature effect on the reaction on the surface reaction rate constant k'_{sr}. The apparent activation energy obtained from Arrhenius plot was around 78 ± 9 kJ/mol for temperatures between 75 and 100 °C. Compensation effects are well described by experimental and simulated data, suggesting that apparent activation energy actually depends on temperature. It was demonstrated the agreement of the model to pseudo-first order rate law when times are in the range of 2–24 h of reaction; moreover our kinetics predicts lower activation energies in pseudo-homogeneous rate laws. The nopol production could not be totally described by the kinetics of its formation reaction at long times; it is partially improved by a semi-empirical deactivation law. It would be necessary to introduce kinetic models that describe also byproduct formation, depolymerization of paraformaldehyde and polymerization in the gaseous phase of HCHO when the experimental setup allows that the vapor phase is in contact with zones below 80 °C.

Acknowledgments

Financial support of Universidad de Antioquia (Suistainability Strategy 2011-2012) is grateful acknowledged. E.A. acknowledges to COLCIENCIAS his doctoral fellowship. The authors acknowledge to professor Consuelo Montes (RIP) for her support in the development of the research.

References

[1] R.E. Kirk, D.F. Othmer, Encyclopedia of Chemical Technology, vol. 26, fourth ed., John Wiley & Sons, New York, 1997.
[2] J.P. Bain, I. Nopol, The reaction of β-pinene with formaldehyde, J. Am. Chem. Soc. 68 (1946) 638–641.
[3] A.L. Villa de P., E. Alarcón, C. Montes de C., Synthesis of nopol over MCM-41 catalysts, Chem. Commun. (2002) 2654–2655.
[4] A.L. Villa de P, E. Alarcón, C. Montes de C, Nopol synthesis over Sn-MCM-41 and Sn-kenyaite catalysts, Catal. Today 107–108 (2005) 942–948.
[5] A. Corma, M. Renz, Water-resistant Lewis-acid sites: carbonyl-ene reactions catalyzed by tin-containing, hydrophobic molecular sieves, ARKIVOC 8 (2007) 40–48.
[6] E. Alarcón, A.L. Villa de P., C. Montes de C., Characterization of Sn- and Zn-loaded MCM-41 catalysts for nopol synthesis, Microporous Mesoporous Mater. 122 (2009) 208–215.
[7] E. Alarcón, A.L. Villa de P., C. Montes de C., Efecto de las condiciones de síntesis hidrotérmica de Sn-MCM-41 en la producción de nopol, Rev. Fac. Ing. Univ. Antioquia 49 (2009) 19–29.
[8] V. Ramaswamy, P. Shah, K. Lazar, A.V. Ramaswamy, Synthesis, characterization and catalytic activity of Sn-SBA-15 mesoporous molecular sieves, Catal. Surv. Asia 12 (2008) 283–309.
[9] M. Selvaraj, Y. Choe, Well ordered two-dimensional SnSBA-15 catalysts synthesized with high levels of tetrahedral tin for highly efficient and clean synthesis of nopol, Appl. Catal. A 373 (2010) 186–191.
[10] E. Alarcón, L. Correa, A.L. Villa de P., C. Montes de C., Nopol production over Sn-MCM-41 synthesized by different procedures – Solvent effects, Microporous Mesoporous Mater. 136 (2010) 59–67.
[11] S. Watanabe, Reaction velocity of the thermal condensation of β-pinene with formaldehyde, J. Chem. Soc. Japan (Kogyo Kagaku Zasshi) 68 (1965) 1622–1623.
[12] L.F. Correa, E. Alarcón, A.L. Villa, Velocidad de reacción empírica para la producción de nopol, Memorias XV Congreso Colombiano de Química, Bogotá, Colombia, Octubre 29–31 de 20, (ISBN: 978-958-98759-0-2).
[13] H.S. Fogler, Elementos de Ingeniería de las reacciones químicas, third ed., Prentice Hall, New Jersey, 2001.
[14] M. Grün, K.K. Unger, A. Matsumoto, K. Tsutsumi, Novel pathways for the preparation of mesoporous MCM-41 materials: control of porosity and morphology, Microporous Mesoporous Mater. 27 (1999) 207–216.
[15] M.A. Vannice, Kinetics of Catalytic Reactions, first ed., Springer Science, New York, 2005.
[16] H. Lynggaard, A. Andreasen, C. Stegelmann, P. Stoltze, Analysis of simple kinetic models in heterogeneous catalysis, Prog. Surf. Sci. 77 (2004) 71–137.
[17] K. Ojha, N.C. Pradhan, A.N. Samanta, Kinetics of batch alkylation of phenol with *tert*-butyl alcohol over a catalyst synthesized from coal fly ash, Chem. Eng. J. 112 (2005) 109–115.
[18] T.L. Gunale, V.V. Mahajani, An insight into Ru/TiO_2 catalyzed wet air oxidation of N-ethylethanolamine in an aqueous solution, Chem. Eng. J. 159 (2010) 17–23.

[19] M.A. Tike, V.V. Mahajani, Kinetics of hydrogenation of palm stearin fatty acid over Ru/Al_2O_3 catalyst in the presence of small quantity of water, Indian J. Chem. Technol. 14 (2007) 52–63.
[20] H. Rojas, G. Borda, J.J. Martínez, J. Valencia, P. Reyes, Liquid phase hydrogenation of citral and intermediaries over $Ir/TiO_2/SiO_2$ catalysts: kinetic study, J. Mol. Catal. A – Chem. 286 (2008) 70–78.
[21] A. Schmidt, R. Schomäcker, Kinetics of 1,5-cyclooctadiene hydrogenation on Pd/α-Al_2O_3, Ind. Eng. Chem. Res. 46 (2007) 1677–1681.
[22] S. Miao, B.H. Shanks, Mechanism of acetic acid esterification over sulfonic acid-functionalized mesoporous silica, J. Catal. 279 (2011) 136–143.
[23] O. Boonthamtirawuti, W. Kiatkittipong, A. Arpornwichanop, P. Praserthdam, S. Assabumrungrat, Kinetics of liquid phase synthesis of tert-amyl ethyl ether from tert-amyl alcohol and ethanol over Amberlyst 16, J. Ind. Eng. Chem. 15 (2009) 451–457.
[24] J. Guo, M. Al-Dahhan, Kinetics of wet air oxidation of phenol over a novel catalyst, Ind. Eng. Chem. Res. 42 (2003) 5473–5481.
[25] P. Beltrame, G. Zuretti, Kinetics of the reaction of toluene with benzyl alcohol over a Nafion–silica composite, Appl. Catal. A: Gen. 283 (2005) 33–38.
[26] S. Abelló, S. Dhir, G. Colet, J. Pérez-Ramírez, Accelerated study of the citral–acetone condensation kinetics over activated Mg–Al hydrotalcite, Appl. Catal. A: Gen. 325 (2007) 121–129.
[27] S.P. Bawane, S.B. Sawant, Reaction kinetics of the liquid-phase hydrogenation of benzonitrile to benzylamine using Raney nickel catalyst, Chem. Eng. J. 103 (2004) 13–19.
[28] G. Reuss, W. Disteldorf, A. Otto, A. Hilt, Formaldehyde, in: Ullmann's Encyclopedia of Industrial Chemistry – Online Edition, Wiley-VCH, Weinheim, 2005, pp. 1–34. doi:10.1002/14356007.a11_619.
[29] F. Sandelin, P. Oinas, T. Salmi, J. Paloniemi, H. Haario, Dynamic modelling of catalytic liquid-phase reactions in fixed beds – kinetics and catalyst deactivation in the recovery of anthraquinones, Chem. Eng. Sci. 61 (2006) 4528–4539.
[30] J.G. Boyles, S. Toby, Kinetics of polymerization of gaseous formaldehyde, J. Polym. Sci. A1 (5) (1967) 1705–1716.